

Substitution of 5-HT_{1A} Receptor Signaling by a Light-activated G Protein-coupled Receptor*

Received for publication, May 25, 2010, and in revised form, July 13, 2010. Published, JBC Papers in Press, July 19, 2010, DOI 10.1074/jbc.M110.147298

Eugene Oh[†], Takashi Maejima^{‡§}, Chen Liu[†], Evan Deneris[†], and Stefan Herlitze^{†§¶}

From the [†]Department of Neurosciences, School of Medicine, Case Western Reserve University, Cleveland, Ohio 44106 and the

[‡]Department of General Zoology and Neurobiology, Ruhr University, Bochum 44780, Germany

Understanding serotonergic (5-HT) signaling is critical for understanding human physiology, behavior, and neuropsychiatric disease. 5-HT mediates its actions via ionotropic and metabotropic 5-HT receptors. The 5-HT_{1A} receptor is a metabotropic G protein-coupled receptor linked to the G_{i/o} signaling pathway and has been specifically implicated in the pathogenesis of depression and anxiety. To understand and precisely control 5-HT_{1A} signaling, we created a light-activated G protein-coupled receptor that targets into 5-HT_{1A} receptor domains and substitutes for endogenous 5-HT_{1A} receptors. To induce 5-HT_{1A}-like targeting, vertebrate rhodopsin was tagged with the C-terminal domain (CT) of 5-HT_{1A} (Rh-CT_{5-HT1A}). Rh-CT_{5-HT1A} activates G protein-coupled inward rectifying K⁺ channels in response to light and causes membrane hyperpolarization in hippocampal neurons, similar to the agonist-induced responses of the 5-HT_{1A} receptor. The intracellular distribution of Rh-CT_{5-HT1A} resembles that of the 5-HT_{1A} receptor; Rh-CT_{5-HT1A} localizes to somatodendritic sites and is efficiently trafficked to distal dendritic processes. Additionally, neuronal expression of Rh-CT_{5-HT1A}, but not Rh, decreases 5-HT_{1A} agonist sensitivity, suggesting that Rh-CT_{5-HT1A} and 5-HT_{1A} receptors compete to interact with the same trafficking machinery. Finally, Rh-CT_{5-HT1A} is able to rescue 5-HT_{1A} signaling of 5-HT_{1A} KO mice in cultured neurons and in slices of the dorsal raphe showing that Rh-CT_{5-HT1A} is able to functionally compensate for native 5-HT_{1A}. Thus, as an optogenetic tool, Rh-CT_{5-HT1A} has the potential to directly correlate *in vivo* 5-HT_{1A} signaling with 5-HT neuron activity and behavior in both normal animals and animal models of neuropsychiatric disease.

Serotonin (5-hydroxytryptamine (5-HT)²) has been demonstrated to play important roles in regulating various physiolog-

ical functions and modulating numerous disease processes. The 5-HT_{1A} receptor regulates 5-HT neuron firing by auto-regulating the release of 5-HT. Receptor activation leads to a decrease in firing via hyperpolarization of the cell membrane (1). In the dorsal raphe, the largest serotonergic nucleus, 5-HT_{1A} is found in cell bodies and dendrites of neurons (2, 3). 5-HT_{1A} receptors have been implicated in a wide variety of physiological and behavioral functions including learning and memory, sexual behavior, and aggression (4–6). Furthermore, 5-HT_{1A} has been implicated in the pathogenesis of anxiety and depression and is thought to be a physiologic target for selective serotonin reuptake inhibitor treatment (7).

Although to date it has been one of the most extensively studied of the serotonin receptors, there is still ambiguity about the normal *in vivo* function of 5-HT_{1A}, dysfunction in the context of disease, and role in therapeutic response. Studies using pharmacologic and genetic manipulations have been enormously useful in defining *in vivo* 5-HT_{1A} function, but of course both approaches have their limitations. Drugs can be applied focally but not spatially contained or targeted to specific cell populations; they also include side effects that can confound analysis. Genetic mutations have the power to be targeted to specific cell types but are constitutionally lost or gained with KOs or transgenics or imprecisely controlled with conditional strategies. Neither approach can be controlled on a second time scale. The ability to modulate 5-HT_{1A} activity in intact, behaving animals with non-invasive techniques would, thus, prove to be a significant advance to a clearer understanding of the role of 5-HT_{1A} and the serotonergic system.

Light-activated G protein-coupled receptors (GPCRs) couple to intracellular signaling pathways in a receptor-specific manner (8). We previously demonstrated that the GPCR, vertebrate rhodopsin (Rh), can be functionally expressed in non-visual cell types to activate downstream targets of G_{i/o} signaling (9). Furthermore, we have shown that Rh can be exogenously expressed in neurons both in primary culture and in intact animals to inhibit neuronal and neural network excitability (9). Based on these findings, we aimed to tailor the properties of Rh to manipulate other GPCR signaling pathways, namely, the 5-HT_{1A}. Here we describe the development of a chimeric light-sensitive GPCR that mimics the intracellular targeting and functional G_{i/o}-linked signaling of wild type 5-HT_{1A}. This receptor, which we call Rh-CT_{5-HT1A}, is able to functionally substitute for endogenous 5-HT_{1A} receptors by exploiting the intracellular trafficking mechanisms used by the endogenous receptors. We show that Rh-CT_{5-HT1A} distributes intra-neuronally to cell membrane sites normally occupied by 5-HT_{1A},

* This work was supported, in whole or in part, by National Institutes of Health Grants RO1 MH062723 (to E. D.), R01 MH081127 (to S. H.), and SBIR R43 MH083302 (to LucCell, Inc.). This work was also supported by National Research Service Award F30 MH084371, Medical Scientist Training Program Training Grant 2T32 GM007250-29, Neurosciences Training Grant 5T32 AG000271-07 (to E. O.), and Japan Society for the Promotion of Science Postdoctoral Fellowships for Research Abroad (to T. M.).

[†]To whom correspondence should be addressed: Dept. of General Zoology and Neurobiology, Ruhr-University, Bochum, Germany. Tel.: 49-234-32-24363; Fax: 49-234-32-14185; E-mail: stefan.herlitze@rub.de.

[‡]The abbreviations used are: 5-HT, 5-Hydroxytryptamine (Serotonin); ANOVA, analysis of variance; CT, C-terminal domain; DRN, dorsal raphe nuclei; GIRK, G protein inwardly rectifying potassium channel; GPCR, G protein-coupled receptor; GTPγS, guanosine 5'-3-O-(thio)triphosphate; mCherry, monomeric Cherry; Rh, vertebrate rhodopsin; DIV, days *in vitro*; GABA, γ-aminobutyric acid; 8OH-DPAT, 8-hydroxy-N,N-dipropyl-2-aminotetralin.

Chimeric GPCR Controls 5-HT_{1A} Signaling by Light

which then allows Rh-CT_{5-HT_{1A}} to induce activation of the same downstream G_{i/o} signaling targets with light stimulus.

EXPERIMENTAL PROCEDURES

Generation of Plasmid Constructs for Transfection and Pseudovirion Production—Rat Rh (RO4) and human 5-HT_{1A} cDNA (GenBank™ accession numbers Z46957 and AF498978) clones were tagged C-terminally with mCherry immediately after the last coding codon using a two-step fusion PCR. Distal primers for Rh-mCherry were 5'-ATCGCTCGAGATGAACGGCACA-GAGGGC-3' and 5'-GCTGATTATGATCTAGAGTCGCG-3'; distal primers for 5-HT_{1A}-mCherry were 5'-ATCGCTCGAGA-TGGATGTGCTCAGCCCTG-3' and 5'-GCTGATTATGATC-TAGAGTCGCG-3'. Primers for the fusion site were 5'-AGCC-AGGTGGCTCCAGCCATGGTGAGCAAGGGCGAG-3' and 5'-CTCGCCCTGCTCACCATGGCTGGAGGCCACTGGCT-3' for RO4-mCherry and 5'-ATTAAGTGTAAAGTCTGCCGC-CAGATGGTGAGCAAGGGCGAG-3' and 5'-CTCGCCCT-TGCTCACCATCTGGCGGCAGAACTTACACTTAAT-3' for 5-HT_{1A}-mCherry. For Rh-CT_{5-HT_{1A}}, the C-terminal domain of human 5-HT_{1A} was appended immediately after the last coding nucleotide of Rh-mCherry by fusion PCR using the 5' distal primer for Rh-mCherry, the 3' distal primer for 5-HT_{1A}-mCherry, and the fusion primers 5'-GCATGGACGAGCTGTACAAGAACAGGACTTTCAAAACGCG-3' and 5'-CGCGTTTGAAAGT-CCTTGTCTTGTACAGCTCGTCCATGC-3'. These fragments were PCR-amplified using the respective distal primers and cloned into the XhoI and NotI sites of pEGFP-N1 (Clontech) to generate HEK cell expression clones. Human 5-HT_{1A} cDNA was purchased from the Missouri S&T cDNA Resource Center (Rolla, MO).

To construct Sindbis virus expression vectors, SinRep(nsP2S⁷²⁶)dSP-EGFP (9) was modified using the gateway vector conversion system (Invitrogen). Briefly, the RfA cassette was cloned into the PmII site of SinRep(nsP2S⁷²⁶)dSP-EGFP to generate a gateway destination vector. Entry clones were generated by cloning of genes of interest into pENTR/D-TOPO or pCR8/GW/TOPO according to manufacturer's protocol (Invitrogen). LR recombination was performed to generate final Sindbis expression clones. Lentivirus expression constructs were made by LR recombination of each entry clone together with pENTR5'/CMVp into pLenti6.4/R4R2/V5-Dest (Invitrogen).

Cell Culture, Virus Production, and Infection—Cell culture and maintenance of human embryonic kidney 293 (HEK293) cells (tsA201 cells) were performed as described previously (10). Cells were transfected with 2 µg of each GPCR DNA and 1 µg of each GIRK channel subunit DNA with Lipofectamine 2000 (Invitrogen) and incubated for 18–24 h before recordings or fixation for immunocytochemistry.

Sindbis pseudovirions were generated as previously described (9). Lentiviral particles were made by cotransfection of each lentivirus expression vector together with pLP1, pLP2, and pLP/VSVG helper plasmids into HEK293T/17 cells (ATCC# CRL-11268) according to Invitrogen protocols. Both Sindbis and lentiviral particles were concentrated by ultracentrifugation at 160,000 × g for 90 min through a 20% sucrose cushion

and resuspended in HBSS. Viral titer was greater than 1 × 10⁸ units per ml and stocked at -80 °C.

Continental culture of hippocampal neurons from P0-P3 rats and mice were performed by a modified Banker sandwich method as described (11, 12). The generation of 5-HT_{1A} KO mice (13, 14) and genotyping methods (15) have been previously described. WT mice (C57BL/6J) were obtained from The Jackson Laboratory (Bar Harbor, ME). Handling and care of mice followed federal guidelines, and experimental methods were approved by the Case Western Reserve University Institutional Animal Care and Use Committee. For neuronal infection, 0.5–5 µl of thawed Sindbis virus suspension was added to cultured hippocampal neurons (9–14 DIV) on coverslips in 24-well plates. GFP expression was detected after 10 h and reached maximal expression after 24 h.

Lentiviral Injections into the Dorsal Raphe Nuclei—Lentivirus expressing Rh-CT_{5-HT_{1A}} was injected into the dorsal raphe nucleus (DRN) of wild type (C57Bl/6J), ePet::YFP or 5-HT_{1A}^{-/-} mice. 3-Week-old mice were anesthetized with 1–2% isoflurane in air delivered from a precision vaporizer (WPI) and mounted onto a stereotactic frame (Narishige). A sagittal incision along the midline was made to expose the cranium, and a burr hole was drilled 4.1 mm from the bregma. The tip of a micropipette attached to a 30-ml syringe was lowered into the dorsal raphe nucleus, and 3–4 µl of the virus was injected. Mice were housed for 7–10 days before performing immunohistochemistry or electrophysiological experiments.

Immunofluorescence, Image Acquisition, and Data Analysis—tsA201 cells were transfected with the indicated DNAs using Lipofectamine 2000, and hippocampal neurons (8–10 DIV) were transfected with using Sindbis viral stocks. HEK cells and neurons were fixed with 4% paraformaldehyde for 10 min and permeabilized with 0.1% Triton X-100 in PBS 18 h and 12 h post-transfection, respectively. Anti-dsRed (Clontech; 1:300) was used to label mCherry tagged receptors, and anti-5-HT_{1A} (Millipore; 1:500) was used to stain endogenous receptor. Anti-MAP-2 (Sigma; 1:500) and anti-Tau-1 (Millipore; 1:200) were used to label dendritic and axonal processes. Cells were blocked with 10% normal goat serum and 3% BSA and incubated with primary antibody overnight at 4 °C. After extensive washes, they were incubated with Alexa 405- and Alexa 546-conjugated secondary antibodies (Molecular Probes) for 30 min at room temperature. Cells were mounted in Prolong Gold antifade medium (Molecular Probes). Images were acquired with a Zeiss LSM 510 confocal microscope using 20× and 40× water objectives and analyzed by using VOLOCITY (Improvision, Lexington, MA) and Zeiss LSM 5 software (Release 3.2). Z-stack images were acquired to image the entire cell and displayed as a projected image or single slice through the center of cell where indicated. For quantification of relative fluorescence intensity, imaging parameters were adjusted so that pixel intensity within neurites did not saturate. The line profile function in the LSM 5 software was used to trace the longest dendrite of each neuron analyzed. Dendrites were identified by both MAP-2 (dendritic marker) and GFP (positive infection) fluorescence. Fluorescence intensity was normalized to maximal intensity of each dendrite. For quantification of fluorescence along dendrite, piecewise linear interpolation was performed of each plot to

Chimeric GPCR Controls 5-HT_{1A} Signaling by Light

normalize the line profile distance to 1000 values between 0.0 and 1.0. Interpolated data were then grouped and plotted as the mean \pm S.E. at each normalized point.

For immunohistology, adult mice were deeply anesthetized before transcardial perfusion with 4% paraformaldehyde in 0.1 M PBS for 20 min. The brain was then removed and fixed in paraformaldehyde for another 2 h at room temperature followed by cryoprotection in 30% sucrose (w/v) overnight at 4 °C. Tissue sections (16–20 μ m) were prepared on a freezing microtome or cryostat and mounted on Superfrost Plus Microscope Slides (Fisher). Fluorescent immunohistochemistry was performed as described (16). Tissue sections were immunolabeled with rabbit anti-GFP (1:1,000, Invitrogen) and then FITC-conjugated secondary antibody (1:200, Jackson ImmunoResearch, West Grove, PA). Fluorescent images were collected using a SPOT RT color digital camera (Diagnostic Instruments, Sterling Heights, MI) attached to an Olympus Optical BX51 microscope (Center Valley, PA).

Electrophysiology and Data Analysis—For GIRK channel recordings in HEK293 cells, human GIRK channel subunits (KCNJ3/5) and light-sensitive GPCRs or 5-HT_{1A} receptor were coexpressed in tsA201 cells. GIRK subunit DNA was purchased from Genecopoeia (Rockville, MD). Cells were cultured and recorded in dark room conditions (red light only) after transfection. GIRK-mediated K⁺ currents were measured and analyzed as described previously (17). Absolute GIRK current was determined by brief application of a low K⁺ solution to abrogate GIRK current: 138 mM NaCl, 2 mM KCl, 2 mM CaCl₂, 1 mM MgCl₂, 10 mM HEPES-NaOH, pH 7.3 (KOH). The difference in current elicited with high K⁺ (external solution) and low K⁺ solutions was determined to be the absolute GIRK current. The external solution was as follows: 20 mM NaCl, 120 mM KCl, 2 mM CaCl₂, 1 mM MgCl₂, 10 mM HEPES-NaOH, pH 7.3 (KOH). Patch pipettes (2–5 megaohms) were filled with internal solution: 100 mM potassium aspartate, 40 mM KCl, 5 mM MgATP, 10 mM HEPES-KOH, 5 mM NaCl, 2 mM EGTA, 2 mM MgCl₂, 0.01 mM GTP, pH 7.3 (KOH). Cells were incubated in external solution containing 1 μ M 9-cis-retinal (Sigma) for 20 min before light stimulation. Cells were visualized using a transilluminated red light (590 nm filter) during experimental manipulations. GTP γ S was added to the internal solution at a final concentration of 0.6 mM where indicated. Solutions containing agonist or low potassium were applied directly onto the recorded cells using a fast-flow perfusion system (ALA Scientific, Farmingdale, NY).

Cultured hippocampal neurons were recorded on days 10–14 *in vitro* 14–20 h after Sindbis virus infection. Extracellular recording solution contained 125 mM NaCl, 2 mM KCl, 10 mM Hepes, 30 mM glucose, 3 mM CaCl₂, and 1 mM MgCl₂, pH 7.3 (NaOH); internal solution contained 97 mM potassium gluconate, 10 mM Hepes, 1 mM potassium-EGTA, 4 mM Mg-ATP, and 0.4 mM Na-GTP pH 7.3 (KOH). Synaptic activity was silenced by adding 10 μ M 6-cyano-7-nitroquinoxaline-2,3-dione (Tocris) and 10 μ M SR 95531 hydrobromide (Gabazine, Tocris). Cells were perfused with 1 μ M 9-cis-retinal (Sigma) for 2 min before light stimulation. 1 μ M 8OH-DPAT (Calbiochem) and 50 μ M baclofen (Sigma) were used in experiments where indicated.

Whole-cell patch clamp recordings of cultured neurons and tsA201 (18) were performed with an EPC9 amplifier (HEKA). Currents were digitized at 10 kHz and filtered with the internal 10-kHz three-pole Bessel filter (filter 1) in series with a 2.9-kHz 4-pole Bessel filter (filter 2) of the EPC9 amplifier. Series resistances were partially compensated between 70 and 90%. Leak and capacitive currents were subtracted by using hyperpolarizing pulses from -60 to -70 mV with the p/4 method.

Brain Slice Recordings—Coronal slices including dorsal raphe (250 μ m thick) were cut from brainstems of the mice 8–12 days after lentivirus injection. Mice were anesthetized with isoflurane and decapitated. The removed brainstem was cooled and sliced in ice-cold solution containing 87 mM NaCl, 75 mM sucrose, 2.5 mM KCl, 0.5 mM CaCl₂, 7 mM MgCl₂, 1.25 mM NaH₂PO₄, 25 mM NaHCO₃, and 20 mM glucose bubbled with 95% O₂ and 5% CO₂ using with a vibratome (VT1000S, Leica). Slices were stored for at least 1 h at room temperature in a recording artificial cerebrospinal fluid containing 124 mM NaCl, 3 mM KCl, 2.5 mM CaCl₂, 1.2 mM MgSO₄, 1.23 mM NaH₂PO₄, 26 mM NaHCO₃, and 10 mM glucose bubbled with 95% O₂ and 5% CO₂. Fluorescent mCherry-positive cells were visually identified under an upright microscope (DMLFSA, Leica) equipped with a monochromator system (Polychrome IV, TILL Photonics) flashing 585-nm excitation light. Whole-cell recordings were made at room temperature in the dark except for using infrared light to target the cell. Slices were preincubated at least 20 min and continuously perfused with the external solution including 25 μ M 9-cis-retinal, 0.025% (\pm)- α -tocopherol (Sigma), 0.2% essentially fatty acid free albumin from bovine serum (Sigma), and 0.1% dimethyl sulfoxide. Patch pipettes (2–4 megaohms) were filled with an internal solution with the composition 140 mM potassium methyl sulfate, 4 mM NaCl, 10 mM HEPES, 0.2 mM EGTA, 4 mM Mg-ATP, 0.3 mM Na-GTP, and 10 mM Tris-phosphocreatine, pH 7.3 (KOH). Membrane currents and voltages were recorded with an EPC10/2 amplifier (HEKA). The signals were filtered at 3 kHz and digitized at 50 kHz. The PatchMaster software (HEKA) was used for the controls of voltage and data acquisition, and off-line analysis was made with Igor Pro 6.0 software (Wavemetrics).

Statistical significance throughout the experiments was tested with ANOVA using Igor 6.0 software (Wavemetrics). S.E. are the mean \pm S.E.

RESULTS

Cloning of Rh-CT_{5-HT1A} and Optimization of the Light Activation Paradigm—Vertebrate Rh and 5-HT_{1A} are G_{i/o}-linked GPCRs belonging to the Class A (rhodopsin-like) family of seven transmembrane domain receptors. Because they both activate G_{i/o}-linked downstream signaling pathways, we hypothesized that we could functionally replace 5-HT_{1A} receptor with a light-sensitive receptor by inducing the subcellular targeting of Rh to copy that of wild type 5-HT_{1A}. We did this by tagging Rh with the C-terminal domain of 5-HT_{1A} receptor (CT), which has been shown to be critical for regulating correct intracellular trafficking of 5-HT_{1A} via its interaction with the Yif1B (19). This receptor, which we call Rh-CT_{5-HT1A}, consists of Rh-tagged C-terminally with mCherry and then with the CT

Chimeric GPCR Controls 5-HT_{1A} Signaling by Light

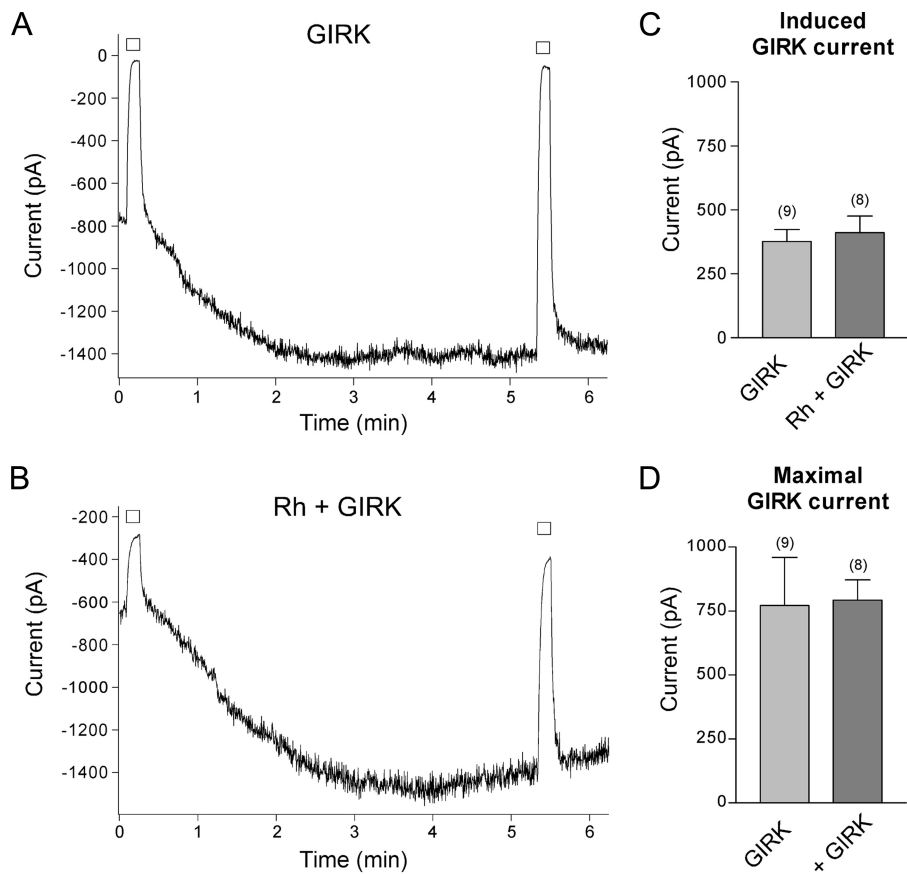


FIGURE 1. Vertebrate rhodopsin does not activate GIRK channels in the absence of light stimulus. HEK293 (tsA201) cells were co-transfected with either GIRQ1/4 subunits alone (A) or GIRQ1/4 and Rh (C), and GIRQ currents were measured at a holding potential of -60 mV. 0.6 mM GTP γ S present in the intracellular recording solution caused constitutive G protein activation and subsequent GIRQ current enhancement. A low K $^{+}$ (2 mM) solution was applied for 10 s (white bars) at 5 s and 5 min after establishment of the whole-cell mode. B, absolute inward currents through GIRQ channels were calculated as the difference between current in normal (high K $^{+}$) extracellular recording solution and low K $^{+}$ (2 mM). The current induced by GTP γ S was calculated as the difference between absolute GIRQ current at 5 min and 5 s. D, maximal GIRQ current was determined by calculating induced GIRQ current at 5 min after gaining access to the intracellular compartment. Quantification of GIRQ current induced by GTP γ S shows no significant difference between HEK293 cells transfected with Rh and GIRQ1/4 or GIRQ1/4 subunits alone. (mean \pm S.E.; $p > 0.05$, ANOVA).

of 5-HT_{1A} (see Fig. 2A). To determine whether this modified receptor retained G_{i/o}-linked GPCR activity, it was co-expressed with human GIRQ1 and -4 subunits in HEK293 cells.

Accurate functional comparison of chimeric receptor with Rh and other GPCRs required modification of fluorescent tag, retinal loading, and recording conditions to improve assay consistency. GFP has been previously used as a CT tag to track functional expression in transgenic animals (20–22). However, when we expressed a similar construct, Rh-EGFP, in HEK293 cells, the amplitude of maximal GIRQ channel activation we observed was at best only ~50% that of untagged or mCherry-tagged versions of Rh (data not shown). Furthermore, the consistency of responses to light stimulus of GFP positive cells was relatively low, 44.44% (12/27). Rh is maximally excited at 485 nm, which coincides almost exactly with the excitation wavelength of EGFP (488 nm). Thus, use of EGFP as a marker for positive transfection could cause inadvertent receptor activation as the rhodopsin apoprotein itself (even in the absence of retinal) exhibits weak activity (23). mCherry is an improved fluorescent tag because it has an excitation/emission profile of

587 nm/610 nm, which lies outside of the absorption spectrum of Rh (24).

Phototransduction by Rh is initiated by the isomerization of the photosensitive pigment, 11-cis-retinal, by light. In the visual system, spent substrate (all-trans-retinal) is recycled by a series of transport and enzymatic reactions (25). HEK cells possess the intrinsic capability to regenerate 11-cis-retinal from all-trans-retinal or other analogs such as 9-cis or 13-cis-retinal but require an exogenous source of retinal (26). Another source of variability was the retinal loading conditions of Rh and variants, which was confounded by the variability of serum used as a culture media supplement. Fetal bovine sera (FBS) contain retinal compounds as evidenced by the ability to activate transfected Rh in HEK293 cells cultured in media made with some but not all lots of FBS. This raised the possibility that ambient light could inadvertently activate the light-sensitive GPCRs. This in turn could lead to a decrease in receptor activity and/or desensitization, potentially confounding the experiments. Considering these complications, cells were kept in the dark after transfection and during experimental procedures. Furthermore, a 20-min preincubation of 1 μ M 9 cis-retinal before recordings was used to yield the most consistent results, regardless of culture media composition. 90.48% (19/21) of mCherry-positive cells responded to light stimulus under these optimized conditions.

In vertebrate rod and cone cells, bleached vertebrate rhodopsin is able to transduce signal, and the pigment may remain in steady state of activation even after light stimulation is eliminated (27–29). Thus, we tested the possibility that light-activated receptors were active in heterologous expression systems even in the absence of light stimulus. This phenomenon could limit the extent of GIRQ current modulation observed and could lead to constitutive, basal increases in G_{i/o} activation. More importantly, because the ultimate goal is to exogenously express Rh-CT_{5-HT1A} in other cell types, this would limit the utility of the light-sensitive receptor as merely expressing it would affect function without light application. HEK293 cells transfected with GIRQ1/4 subunits alone (Fig. 1A) or co-transfected with Rh (Fig. 1C) were analyzed with GTP γ S (a non-hydrolyzable GTP analog) in the intracellular recording solution. GTP γ S caused constitutive G protein activation and gradually led to maximal GIRQ current induction. The absolute

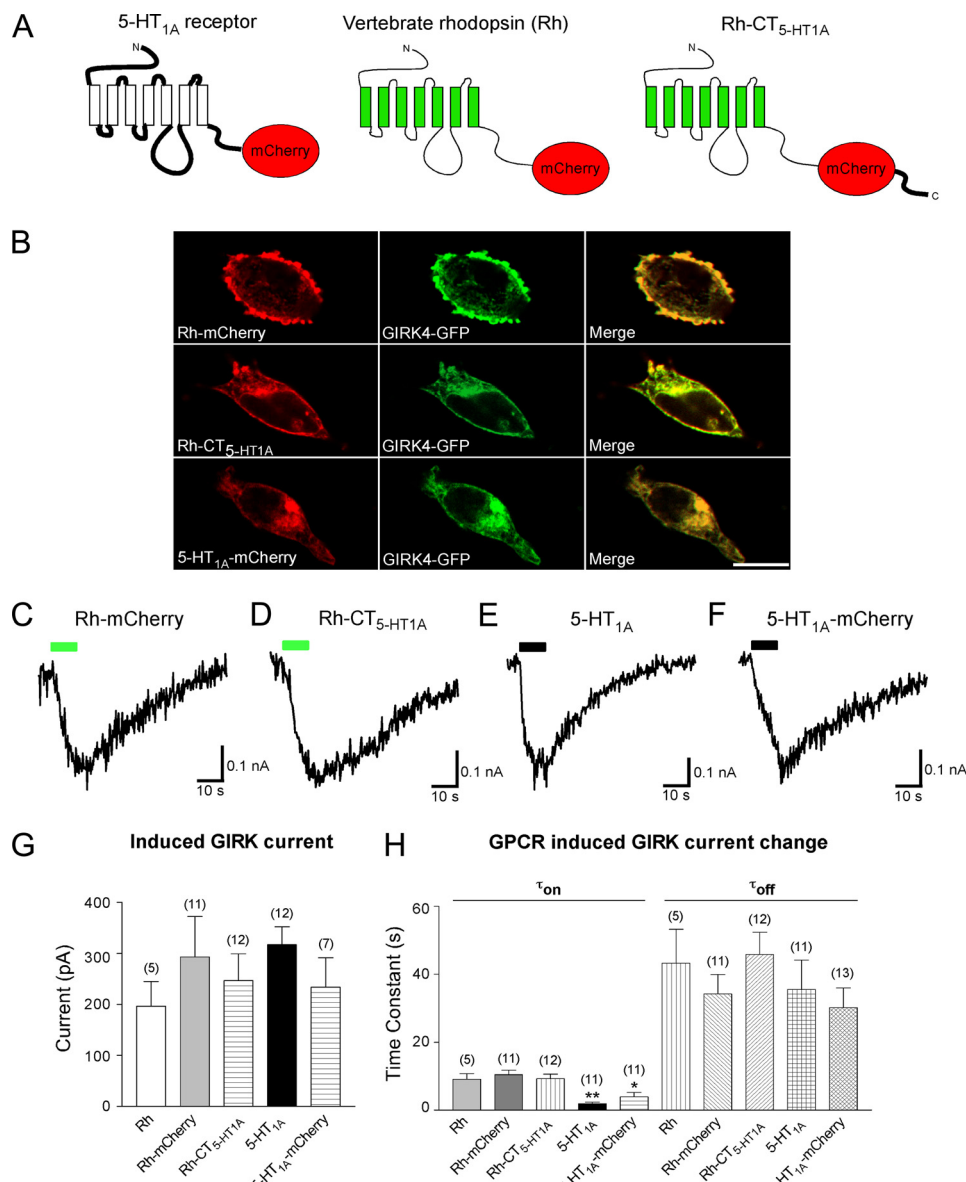


FIGURE 2. Functional expression and characterization of Rh-CT_{5-HT1A} in HEK293 cells. *A*, shown are schematic representations of GPCRs C-terminal-tagged with mCherry used for exogenous expression. The chimera Rh-CT_{5-HT1A} contains the C-terminal domain of human 5-HT_{1A} receptor after the fluorescent tag. *B*, colocalization of GPCRs with GIRK channels exogenously expressed in HEK293 cells. Cells were co-transfected with mCherry tagged receptors, GIRK1 subunit, and GIRK4 subunit tagged N-terminally with EGFP. GPCRs (*left*, red) and GIRK1/4 (*center*, green) channels target efficiently to the cell membrane. *Right*, overlay of *left* and *right* panels shows colocalization of transfected GPCRs and GIRK channels indicated by a yellow color (*scale bar* = 10 μ m). Time course of GPCR-induced GIRK current increase demonstrates that the increase in GIRK current by Rh-mCherry (*C*) and Rh-CT_{5-HT1A} (*D*) in response to a 10-s light pulse of 485 nm (*green bars*) is comparable with the GIRK current increase mediated by 5-HT_{1A} (*E*) or 5-HT_{1A}-mCherry (*F*) when activated by 10 s application of 8OH-DPAT (1 μ M) (*black bars*). GIRK currents were measured at a holding potential of -60 mV. *G*, average light and agonist-induced GIRK current increase is shown. Light-sensitive GPCRs were activated with a 10-s light pulse (485 nm), and 1 μ M 8OH-DPAT was applied to cells transfected with 5-HT_{1A} receptors. *H*, shown is a comparison of the time constants of the GPCR-induced GIRK current changes before and after GPCR activation. Throughout the experiments the number in parentheses indicates the number of experiments and statistical significance as indicated (mean \pm S.E.; * indicates activation time constant was significantly different from Rh, $p < 0.05$; ** indicates activation time constant was significantly different from Rh, $p < 0.001$, ANOVA).

GIRK current was assessed by a short application of low K⁺ (2 mM), eliminating the inward K⁺ current. The GIRK current was then calculated as the difference between current immediately before (high K⁺) and during the low K⁺ treatment. The GIRK currents induced by GTP γ S were not significantly different for HEK cells transfected with Rh and GIRK (410.919 ± 65.217 pA

($n = 8$)) versus GIRK subunits alone (375.958 ± 47.104 pA ($n = 9$)) (Fig. 1*B*), indicating that there was no appreciable activation of GIRK by Rh without light stimulus. Furthermore, the maximal GIRK current revealed by GTP γ S was comparable in cells transfected with GIRK (771.722 ± 181.719 pA ($n = 9$)) or Rh with GIRK subunits (792.455 ± 79.213 pA ($n = 8$)) (Fig. 1*D*), suggesting that Rh co-expression did not interfere with GIRK expression level or targeting.

Expression Pattern and Function of Rh-CT_{5-HT1A} Resembles Fluorescently Tagged 5-HT_{1A} in HEK Cells— mCherry-tagged versions of Rh, 5-HT_{1A}, and Rh-CT_{5-HT1A} were cloned into mammalian expression vectors (Fig. 2*A*). The determinants of G protein specificity and subcellular targeting are presumably contained within the intracellular domains of GPCRs. Based on this assertion, two different chimeric receptors were generated. The first consisted of Rh tagged C-terminally with mCherry and then the CT domain of 5-HT_{1A} (Rh-CT_{5-HT1A}). The CT domain of 5-HT_{1A} has been shown to be necessary for its dendritic targeting via interaction with a putative ER/Golgi trafficking protein, Yif1B (19). The second was a mutant Rh receptor in which the intracellular domains were exchanged for those of 5-HT_{1A} receptor. The rationale for this GPCR was that extracellular and transmembrane domains of Rh were retained, thus preserving responsiveness to light, but the intracellular domains of 5-HT_{1A} would induce subcellular targeting and G protein coupling like 5-HT_{1A}. The exact Rh residues retained and domain borders were analogous to the Rh/ β 2-adrenergic and Rh4/ α 1-adrenergic receptors generated by the Khorana and co-workers (30) and Deisseroth

and co-workers (31). However, this receptor revealed uncharacteristic activation kinetics and was constitutively active once light was applied (data not shown). We, therefore, did not perform a more precise analysis of this chimeric receptor but concentrated on the characterization of Rh-CT_{5-HT1A}.

Chimeric GPCR Controls 5-HT_{1A} Signaling by Light

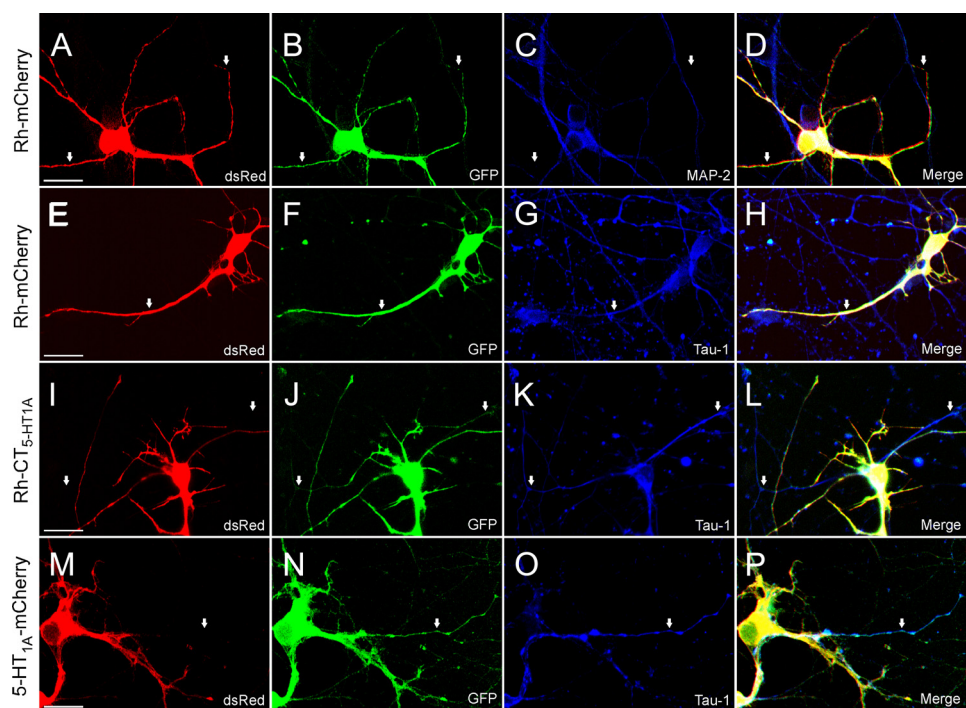


FIGURE 3. The C-terminal domain of 5-HT_{1A} is sufficient to induce targeting of vertebrate rhodopsin somatodendritically in neurons. Confocal immunofluorescence images were taken of cultured rat hippocampal neurons (8 DIV) infected with Sindbis virus driving expression of Rh-mCherry (A–H), Rh-CT_{5-HT1A} (I–L), and 5-HT_{1A}-mCherry (M–P). All Sindbis virus vectors also induced expression of EGFP (B, F, J, and M) under the control of a second subgenomic promoter. Neurons were stained with anti-dsRed antibody (A, E, I, and M) to delineate the distribution of mCherry-tagged receptors and co-labeled with the dendritic marker, MAP-2 (C), or axonal marker, Tau-1 (G, K, and O). Rh-mCherry targets to both axons and dendrites in cultured neurons. Neurons infected with Rh-mCherry virus showed processes with dsRed (A), GFP (B), and MAP-2 (C) staining. Rh-mCherry and GFP were also found in processes that lack MAP-2 expression, suggesting that both proteins are targeted to axons (O). These processes are labeled by white arrows. D, overlay of dsRed, GFP, and MAP-2 staining shows colocalization pattern. Rh-mCherry targeting to axons was revealed by the presence of processes colabeled with anti-dsRed (E) and anti-Tau-1 (G) antibodies. H, overlay of dsRed, GFP, and Tau-1 labeling shows colocalization. The white arrow points to the Rh-mCherry-, GFP-, and Tau-1-positive axon. Rh-CT_{5-HT1A} (I) expressed in hippocampal neurons is present in dendrites but is not targeted to GFP-positive (J) and Tau-1-positive (K) processes. White arrows mark these axons. L, overlay of dsRed in neurons infected with Rh-CT_{5-HT1A} virus shows colocalization of Tau-1-positive and GFP-positive but not Rh-CT_{5-HT1A} processes. 5-HT_{1A}-mCherry (M) also is not targeted to GFP-positive (N) and Tau-1-positive (O) processes. White arrows mark one of these axons. P, overlay of dsRed, GFP, and Tau-1 images shows colocalization of Tau-1- and GFP-positive but 5-HT_{1A}-mCherry negative processes. 10, 12, and 8 neurons expressing Rh-mCherry, Rh-CT_{5-HT1A}, and 5-HT_{1A}-mCherry, respectively, were analyzed. The scale bar represents 20 μ m. Images are representative z-stack images projected to two dimensions.

When co-transfected into HEK293 cells, exogenously expressed Rh-mCherry, Rh-CT_{5-HT1A}, and 5-HT_{1A}-mCherry targeted efficiently to the cell membrane and colocalized with GIRK channel subunits (Fig. 2B). Functionally, Rh-mCherry and Rh-CT_{5-HT1A} were able to activate GIRK current when exposed to light at 485 nm (Figs. 2, C and D). The extent of GIRK activation was not significantly different from untagged Rh and was similar to responses induced in tagged and untagged 5-HT_{1A} receptors (Fig. 2, E and F) by the selective 5-HT_{1A} agonist, 8OH-DPAT (Fig. 2G). It is important to note that the GIRK current induction for all GPCRs tested is similar to that induced by GTP γ S (Fig. 1B), suggesting that both agonist and light application caused near maximal induction of GIRK for 5-HT_{1A} and light-sensitive receptors, respectively. The time constants for onset of GIRK channel activation and deactivation were also similar between Rh, Rh-CT_{5-HT1A}, and 5-HT_{1A} ($\tau_{on} \approx 2\text{--}10$ s, $\tau_{off} \approx 30\text{--}50$ s, Fig. 2H), although activation of 5-HT_{1A} and 5-HT_{1A}-mCherry were significantly faster ($\tau_{on} = 1\text{--}2$ s) than the light-activated receptors

($\tau_{on} \approx 9\text{--}10$ s). The kinetics of inactivation for all GPCRs tested were not significantly different, suggesting that the addition of mCherry and CT tags to Rh does not interfere with function.

Subcellular Targeting of Rh-CT_{5-HT1A} Resembles That of 5-HT_{1A}— Exogenous expression of Rh targets to both somatodendritic and presynaptic sites when expressed in rat hippocampal neurons (9). We confirmed this by immunolabeling neurons infected with Sindbis virus driving the expression of Rh-mCherry and also EGFP under the control of a second subgenomic promoter. GFP was expressed throughout the entire cell and proved to be a valuable tool for identifying and matching axons, dendrites, and soma of infected neurons. Rh-mCherry (Fig. 3A) colocalized with the dendritic marker, MAP-2 (Fig. 3C), but was also expressed in processes that were presumably axons because they were GFP-positive (Fig. 3B) but lacked MAP-2 labeling (Fig. 3, C and D). To confirm this, neurons were stained with anti-Tau-1 antibody (axonal marker), and we observed Rh-mCherry fluorescence that coincided with processes labeled by Tau-1 (Fig. 3, E–H). This indicated that Rh targeted both to axons and dendrites, confirming our previous findings (9). In contrast, virally expressed

5-HT_{1A}-mCherry localized somatodendritically in neurons (Fig. 3, M–P), which is consistent with the *in vivo* distribution of 5-HT_{1A} observed in serotonergic neurons (2, 3, 32). Likewise, Rh-CT_{5-HT1A} showed an analogous intracellular trafficking pattern (Fig. 3, I–L). No dsRed+/GFP+/MAP-2 negative processes were seen in neurons infected with 5-HT_{1A} and Rh-CT_{5-HT1A} viruses. Rh-CT_{5-HT1A} and 5-HT_{1A} fluorescence was absent from the axonal processes of positively infected neurons (Tau-1+/GFP+) at described expression conditions. Axonal Rh-CT_{5-HT1A} was only observed when the receptor was expressed at very high levels by using 2–10-fold higher titer virus and allowing Sindbis infection to occur for greater than 24 h (data not shown). At these conditions, toxicity effects and cell death were observed most likely due to inhibition of host protein synthesis by excessive virally driven expression (33). Axonal targeting and toxicity were similarly observed with high expression of wild type 5-HT_{1A}. Taken together, the data show that the CT of 5-HT_{1A} is sufficient to promote somatodendritic

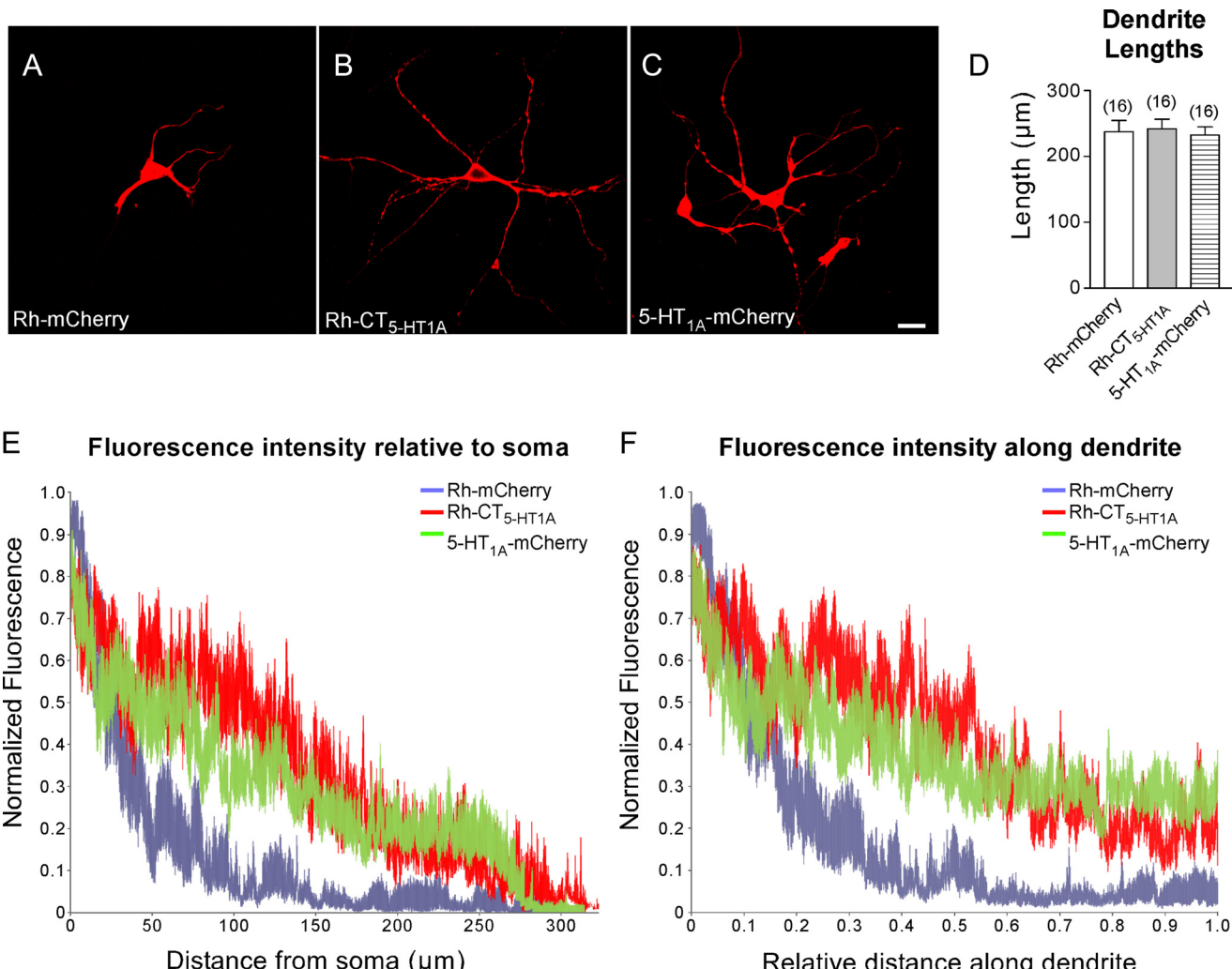


FIGURE 4. The C-terminal domain of 5-HT_{1A} receptor promotes distal targeting within dendrites of hippocampal neurons. Confocal images were taken of cultured rat hippocampal neurons (8 DIV) infected with Sindbis virus driving expression of Rh-mCherry (A), Rh-CT_{5-HT1A} (B), and 5-HT_{1A}-mCherry (C). These neurons were immunolabeled with anti-dsRed (red) and anti-MAP-2 (not shown) antibodies to enhance and delineate mCherry tagged receptors and dendrites, respectively. Images taken at 20× magnification reveal that dsRed fluorescence is observed much more distally from the soma for neurons expressing Rh-CT_{5-HT1A} (B) and 5-HT_{1A}-mCherry (C) when compared with neurons expressing Rh-mCherry (A). E, normalized fluorescence of the longest dendrite of a given neuron was quantified as a function of distance from the soma. Rh-CT_{5-HT1A} (red) and 5-HT_{1A}-mCherry (green) (mean ± S.E.; n = 16). F, Rh-CT_{5-HT1A} and 5-HT_{1A}-mCherry target further along the extent of dendrites. Normalized fluorescence of the longest dendrite was plotted against normalized dendritic length. The length of each dendrite analyzed was normalized from 0 to 1.0 by piecewise linear interpolation. Interpolated data were pooled, and the mean ± S.E. was plotted against normalized distance (n = 16; p > 0.05, ANOVA).

trafficking away from axons in an analogous manner to wild type 5-HT_{1A}.

Another similarity between 5-HT_{1A}-mCherry and Rh-CT_{5-HT1A} was their efficient targeting to the distal ends of dendrites. In comparison to Rh-mCherry (Fig. 4A), 5-HT_{1A}-mCherry and Rh-CT_{5-HT1A} fluorescence is observed much further away from the soma (Fig. 4, B and C). To quantify dendritic fluorescence distributions, neurons infected with Sindbis virus were stained with anti-dsRed to enhance the mCherry signal and minimize bleaching artifacts present by tracking mCherry fluorescence alone. Neurons were also stained with anti-MAP2 antibody to label dendrites. The longest dendrite of infected cells (MAP2+/GFP+) were analyzed in a similar way as described previously (19). Normalized fluorescence was quantified with respect to both absolute distance from the soma (Fig. 4E) and relative distance along the dendrite (Fig. 4F), showing that 5-HT_{1A}-mCherry and Rh-CT_{5-HT1A} are present even at

the distal ends of all dendrites. However, Rh-mCherry fluorescence decays significantly faster along the length of the dendrite, with most of the appreciable fluorescence restricted to the proximal half of the dendrite. The difference in fluorescence distribution is not due to effects on neuronal morphology as the lengths of the dendrites examined were not statistically different between groups (Fig. 4D). Thus, CT of 5-HT_{1A} promotes distal targeting and is sufficient to drive the trafficking of Rh-CT_{5-HT1A} analogously to wild type 5-HT_{1A} receptor.

Rh-CT_{5-HT1A} Is Functional in Cultured Hippocampal Neurons and Competitively Inhibits Targeting of Endogenous 5-HT_{1A} Receptor to Functional Sites—A consequence of G_{i/o}-linked signaling in neurons is the activation of GIRK channels, which are predominantly expressed in dendrites (34). GIRK channel activation causes an efflux of K⁺ resulting in hyperpolarization and subsequent decrease in action potential firing. Therefore, we tested the ability of Rh-CT_{5-HT1A} to activate G_{i/o}

Chimeric GPCR Controls 5-HT_{1A} Signaling by Light

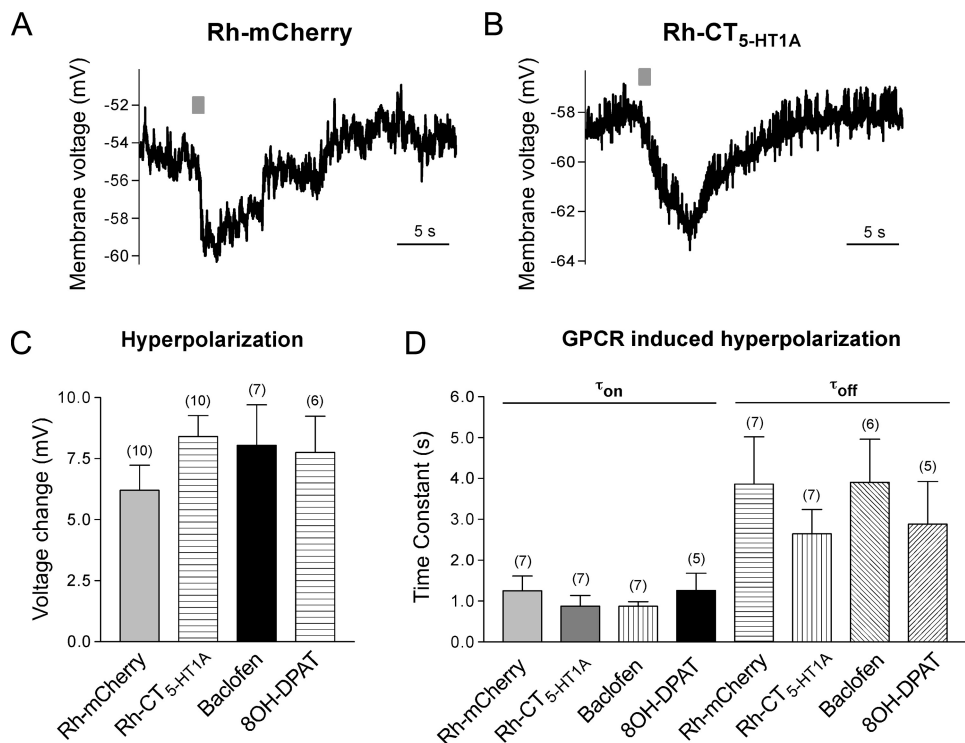


FIGURE 5. Rh-CT_{5-HT1A} induces membrane hyperpolarization in rat hippocampal neurons with light stimulus. *A*, voltage change induced by Rh-mCherry in cultured hippocampal neurons (14 DIV) during a 1-s pulse of 485 nm light is shown. *B*, Rh-CT_{5-HT1A} induced hyperpolarization of hippocampal neurons (14 DIV) by 1-s pulse of 485-nm light is shown. A light-activated receptor-induced voltage change is comparable with agonist induced, G_{i/o}-linked GPCR activation. *C*, shown is average hyperpolarization induced by a 1-s light stimulus (Rh-mCherry and Rh-CT_{5-HT1A}), application of 50 μ M baclofen, or application of 1 μ M of 8OH-DPAT in cultured rat hippocampal neurons (10–14 DIV). For recordings with light stimulus, neurons were infected with Sindbis virus, driving expression of corresponding GPCR. Agonist-induced responses were determined in uninfected neurons. *D*, shown is the time course of GPCR (Rh-mCherry, Rh-CT_{5-HT1A}, GABA_B, or 5-HT_{1A})-induced hyperpolarization and recovery from hyperpolarization after switching off the light or washing out agonist (mean \pm S.E.; average change in membrane potential induced and activation and inactivation time constants were not significantly different from each other, $p > 0.05$, ANOVA).

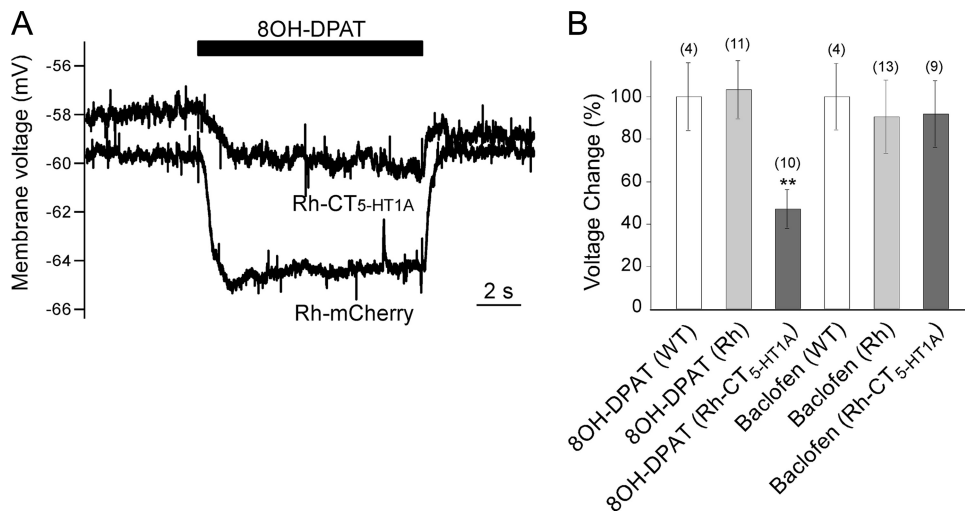


FIGURE 6. Rh-CT_{5-HT1A} replaces endogenous 5-HT_{1A} receptors in hippocampal neurons. Rh-CT_{5-HT1A} but not Rh-mCherry decreases endogenous 5-HT_{1A}-induced hyperpolarization without affecting GABA_B responses. *A*, extent of membrane hyperpolarization induced by 5-HT_{1A} activation is decreased in neurons expressing Rh-CT_{5-HT1A} but not Rh-mCherry. Cultured rat hippocampal neurons (21–22 DIV) were infected with Sindbis virus, driving the expression of Rh-mCherry or Rh-CT_{5-HT1A}. Voltage changes induced by a 10-s application of the 5-HT_{1A} agonist, 8OH-DPAT (1 μ M), in the presence of Rh-CT_{5-HT1A} (top) and Rh-mCherry (bottom) are shown. *B*, relative changes in membrane voltage for 5-HT_{1A} (8OH-DPAT) and GABA_B (baclofen) activation in the absence or presence of Rh-CT_{5-HT1A} and Rh-mCherry compared with the agonist-induced responses in uninfected (WT) cells (mean \pm S.E.; **, $p < 0.01$, ANOVA).

signaling and induce hyperpolarization in a neuronal context. mCherry-tagged Rh (Fig. 5A) as well as the Rh-CT_{5-HT1A} (Fig. 5B) caused a 8–9-mV membrane hyperpolarization (postsynaptic effect) in response to a 1-s light pulse. Hyperpolarization was sustained for the duration of longer (10 s) light stimulus protocols, and cells showed rapid reversal of membrane voltage change after the light was turned off. Uninfected hippocampal neurons were also assessed for their ability to respond to baclofen, a GABA_B agonist that served as a positive control for G_{i/o} activation, and the selective 5-HT_{1A} agonist, 8OH-DPAT. For quantification of biophysical properties, a 1-s light or agonist application was used that was long enough to induce maximal activation of GPCR and induce hyperpolarization but short enough so that GPCR desensitization was not observed. The resulting change in membrane voltage for Rh-mCherry and Rh-CT_{5-HT1A} stimulated by light was not significantly different from neuronal responses to activation of endogenous GABA_B or 5-HT_{1A} receptors (Fig. 5C). The time constants for hyperpolarization and recovery by GPCR activation in neurons were much faster than in HEK293 cells (Fig. 5, *D* versus *H*). This is most likely due to the effect of proteins endogenous to neurons, such as RGS proteins, which potentiate the GTPase activity of G proteins.

Rh-CT_{5-HT1A} contains protein sequence for the interaction with the trafficking machinery normally used by endogenous 5-HT_{1A} receptors. This allows analogous targeting as 5-HT_{1A} but also induces a dominant negative effect because Rh-CT_{5-HT1A} could presumably compete to interact with the same intracellular trafficking proteins (Fig. 6). Hyperpolarization induced by 8OH-DPAT in hippocampal neurons expressing Rh-CT_{5-HT1A} was decreased to 47% \pm 9.2 ($n = 10$) of the non-transfected neuron responses recorded in parallel (Fig. 6). Rh-mCherry expression did not

Chimeric GPCR Controls 5-HT_{1A} Signaling by Light

affect 8OH-DPAT responses ($103.5\% \pm 13.6$ of uninfected neuron ($n = 11$)), indicating that neither viral infection nor exogenous expression of GPCRs affects endogenous 5-HT_{1A} responses. This effect is consistent with the experiments showing that co-expression of the CT reduces 5-HT_{1A} in distal dendrites in cultured neurons (19). Application of baclofen resulted in comparable hyperpolarization for uninfected *versus* Sindbis virus-treated neurons (Rh-mCherry = $90.8\% \pm 17.3$ of uninfected neuron ($n = 13$); Rh-CT_{5-HT1A} = $92.1\% \pm 15.6$ of uninfected neuron ($n = 9$)), ruling out the possibility that virus application interrupted targeting and expression for all endogenous GPCRs.

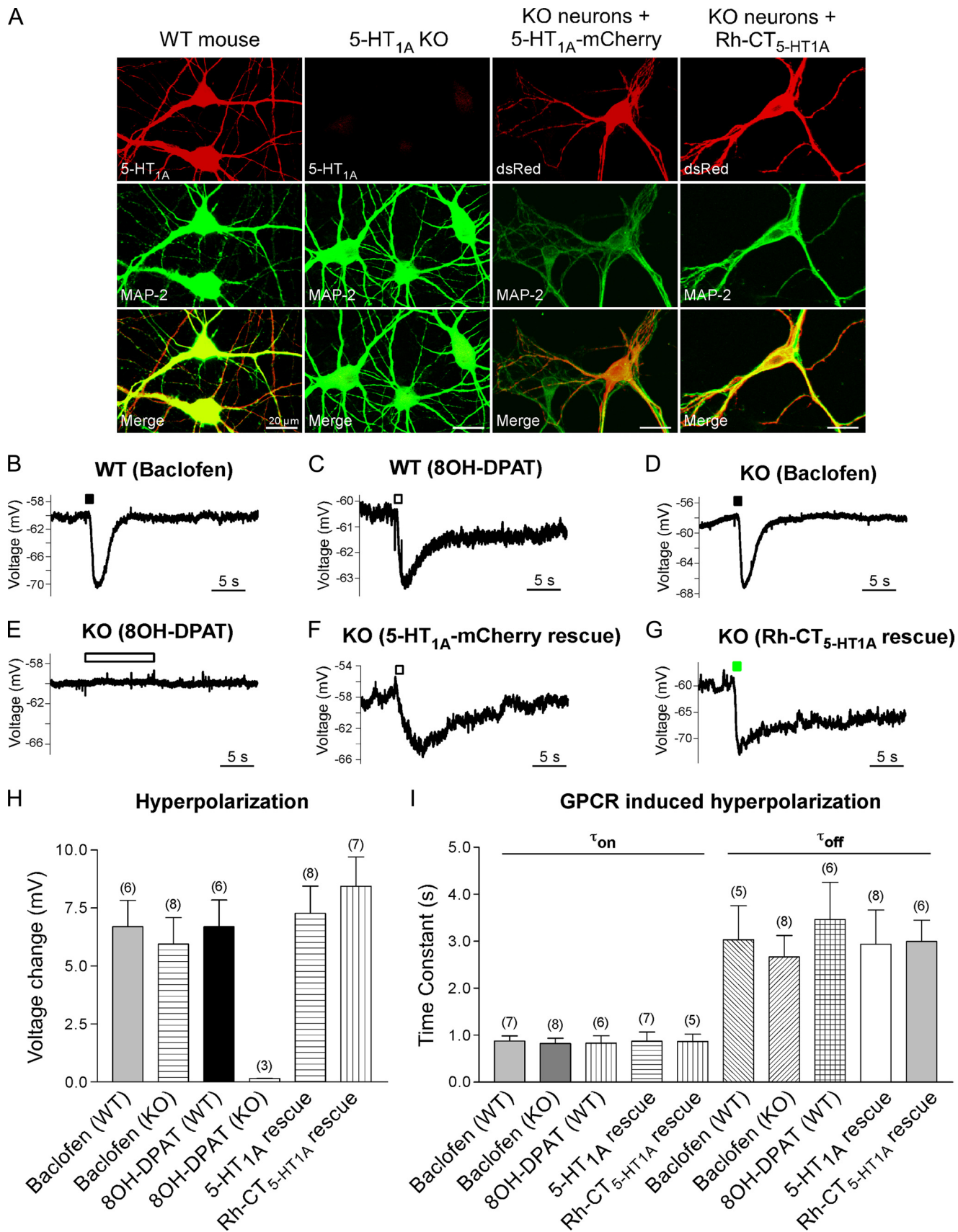
Rh-CT_{5-HT1A} Compensates for the Loss of 5-HT_{1A} Signaling in Cultured Hippocampal Neurons of 5-HT_{1A} Null Mice—To demonstrate that Rh-CT_{5-HT1A} could functionally substitute for 5-HT_{1A} receptors, we sought to determine whether Rh-CT_{5-HT1A} could functionally “rescue” 5-HT_{1A} signaling in neurons from 5-HT_{1A} KO mice. As expected, 5-HT_{1A} immunostaining was absent from neurons from 5-HT_{1A} null mice (13), but hippocampal neurons of wild type mouse showed robust staining throughout dendrites (Fig. 7A). Functionally, the application of $1 \mu\text{M}$ 8OH-DPAT (5-HT_{1A} agonist) onto neurons of KO mice failed to elicit a hyperpolarization response, even with longer agonist applications (10 s) (Fig. 7E). WT mouse neurons hyperpolarized when exposed to $1 \mu\text{M}$ 8OH-DPAT with a comparable response to what was seen in hippocampal neurons cultured from wild type rats (Fig. 7, C and H, *versus* Fig. 5C). The response to baclofen remained intact in the KO neurons, suggesting that the mutation is specific to 5-HT_{1A} and does not affect G_{i/o} signaling broadly (Fig. 7, D and H). 5-HT_{1A}-mCherry and Rh-CT_{5-HT1A} expressed by Sindbis virus vectors localized to the dendrites of KO neurons (Fig. 7A). The hyperpolarization defect in KO neurons was rescued by exogenous expression of both 5-HT_{1A}-mCherry (with agonist application, Fig. 7D) and Rh-CT_{5-HT1A} (with light, Fig. 7G). The loss of function phenotype was completely compensated for, as activation of exogenously expressed 5-HT_{1A} (7.270 ± 1.175 ($n = 8$)) and Rh-CT_{5-HT1A} (8.437 ± 1.271 ($n = 7$)) was indistinguishable from wild type mouse neuron response to 8OH-DPAT.

Rh-CT_{5-HT1A} Functionally Substitutes for 5-HT_{1A} Signaling in Dorsal Raphe Nuclei Neurons in Brain Slices from 5-HT_{1A} Null Mice—We next wanted to demonstrate if Rh-CT_{5-HT1A} was capable of modulating serotonergic neurons of the dorsal raphe compared with endogenous 5-HT_{1A}. Again, these neurons are important neural regulators for the generation of anxiety and depression. Lentivirus expressing Rh-CT_{5-HT1A} was stereotactically injected into the DRN of ePet::YFP or 5-HT_{1A}^{-/-} mice. As indicated in Fig. 8A, Rh-CT_{5-HT1A} was expressed in 5-HT neurons (labeled with YFP in ePet::YFP mice) and revealed a punctate distribution most prominently in the soma. Notably, Rh-CT_{5-HT1A} was absent from (YFP+) long processes most likely representing axons of 5-HT neurons. We next determined if Rh-CT_{5-HT1A} could rescue the phenotype in serotonergic neurons of 5-HT_{1A} KO mice. Similar to what was observed in cultured hippocampal neurons, application of the 5-HT_{1A} agonist, 8OH-DPAT (1 μM), onto brainstem slices failed to elicit a hyperpolarization response in the dorsal raphe

nucleus neurons of KO mice (data not shown). This defect can be rescued by expression of Rh-CT_{5-HT1A} and subsequent activation by light (Fig. 8, B–F). Light stimulus in these neurons caused a decrease in spontaneous action potential firing rate (Fig. 8D). In 10 of 15 cells expressing Rh-CT_{5-HT1A}, the interspike interval was increased in response to a 3-s light stimulus on average from 202 ± 21 ms ($n = 10$) to 313 ± 58 ms and returned to 207 ± 25 ms 13–16 s after cessation of light application (Fig. 8, E and F). The change in firing rate could be attributed to enhancement of K⁺ conductance (most likely mediated by GIRK channels) revealed by increased inward rectification with light (Fig. 8, B and C). Eliciting light responses in brainstem slices required sufficient 9-cis-retinal loading with fatty acid free-BSA-supplemented extracellular solution, facilitating retinal delivery as previously suggested (35). These results indicate that Rh-CT_{5-HT1A} can functionally replace 5-HT_{1A} in the neurons of the dorsal raphe nucleus.

DISCUSSION

Various strategies have been developed to control GPCRs and G protein pathways to dissect the function *in vitro* and *in vivo*. Receptors activated solely by synthetic ligands (RASSL) (36) and designer receptors exclusively activated by designer drugs (DREADDs) (37) are GPCRs that are activated by organic compounds but not by the endogenous ligands such as serotonin or acetylcholine. The basic idea is to use these GPCRs to control the corresponding intracellular pathway by a drug, which specifically only activates the modified GPCR. RASSLs and DREADDs have been used successfully *in vitro* and *in vivo* and have the potential to study GPCR function in a tissue- and cell type-specific manner (38). However, for the investigation of fast spatial-temporal control of GPCRs, for example in brain slice preparations or *in vivo* recordings, the application of chemical compounds to activate the GPCR is slow and almost irreversible. It is difficult to control the ligand concentration in particular in brain tissues, where the chemical compound has to diffuse through various cellular layers and can not be washed out. As a consequence of continuous ligand application, receptor desensitization may occur, and precisely controlled repetitive stimulation of the GPCR pathway is not possible. Therefore, light-activated GPCRs became of interest to us for controlling signaling events in particular in neurons (9, 39). In our first approach we used vertebrate Rh to control the pre- and postsynaptic G_{i/o} signaling in cultured neurons and the embryonic chicken spinal cord. We now became interested in developing this GPCR further. We engineered a chimeric light-activated receptor that targets and functions in 5-HT_{1A} receptor signaling domains. With the addition of mCherry and the CT domain of 5-HT_{1A}, vertebrate Rh retains its ability to activate G_{i/o}-coupled signaling, causes subsequent GIRK channel activation, and induces membrane hyperpolarization. When expressed in neurons, Rh-CT_{5-HT1A} traffics to somatodendritic compartments and to distal dendritic segments, where endogenous and exogenously expressed 5-HT_{1A} receptors are found and functionally substitutes for the missing 5-HT_{1A} receptors in both cultured hippocampal neurons and neurons of the dorsal raphe in hindbrain slices from HT_{1A} KO



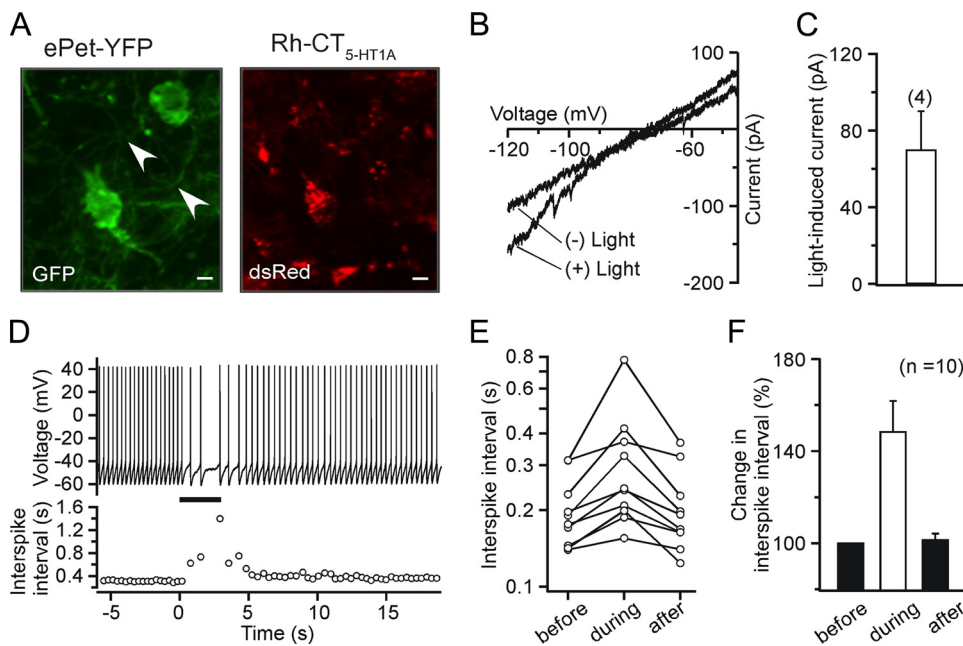


FIGURE 8. Rh-CT_{5-HT_{1A}} compensates for loss of 5-HT_{1A}-mediated signaling of neurons in the dorsal raphe nuclei of 5-HT_{1A} KO mice. *A*, functional expression of Rh-CT_{5-HT_{1A}} in 5-HT neurons of the dorsal raphe is shown. Intracranial injections into the dorsal raphe were performed on ePet::YFP transgenic mice. A lentiviral vector drives the expression of Rh-CT_{5-HT_{1A}} under the control of a CMV promoter (*left*). YFP expressed under the control of a serotonergic-specific promoter, ePet-1, labels 5-HT neurons (*right*). Punctate distribution of Rh-CT_{5-HT_{1A}} is observed in neurons 9 days after injection. Dorsal raphe slices were stained with anti-GFP antibody to amplify the YFP signal. Arrowheads on the *left* indicate neuronal processes, which are YFP-positive but do not express mCherry. Rh-CT_{5-HT_{1A}} expression rescues loss-of-function phenotype in 5-HT neurons of KO mice. *B*, current traces elicited in DRN neurons from 5-HT_{1A} KO mice expressing Rh-CT_{5-HT_{1A}} by a voltage ramp from -120 to -45 mV before and after light activation indicate that 490-nm light pulses increase the membrane currents (most likely mediated by GIRK). *C*, shown is quantification of the light-induced current measured at -120 mV. *D*, top, spontaneous action potential firing of DRN neurons from 5-HT_{1A} null mice expressing Rh-CT_{5-HT_{1A}} is reduced by a 3-s light pulse (490 nm). Bottom, during the light pulse the interspike interval is increased during the light pulse and decreases to resting levels once the light switched off. *E*, plot of the interspike interval for a single experiments of DRN neurons from 5-HT_{1A}^{-/-} mice expressing Rh-CT_{5-HT_{1A}} before, during, and after a 3-s, 490-nm light pulse (*n* = 10). *F*, percent change of the interspike interval for 5-HT_{1A}^{-/-} DRN neurons expressing Rh-CT_{5-HT_{1A}} before, during, and after a 3-s, 490-nm light pulse (*n* = 10).

mice. Thus, our results suggest that Rh-CT_{5-HT_{1A}} can act in place of endogenous 5-HT_{1A} receptor.

In developing Rh-CT_{5-HT_{1A}}, we have gained some important understanding for using light-activated GPCRs to control specific GPCR pathways. We learned that the intracellular trafficking of Rh can be directed to specific subcellular domains by the addition of critical targeting domains of other GPCRs. The successful application of this type of strategy may depend on the presence of specific binding motifs on the donor receptor in addition to the targeting tag. Our efforts to further replace the intracellular domains of Rh using the corresponding 5-HT_{1A} receptor domains produced a light-activated chimeric GPCR

with unusual activation and inactivation kinetics (data not shown). The reason for the altered receptor kinetics will be investigated biophysically in future studies and may shed additional light onto the coupling between GPCR, G protein, and the intracellular signaling cascade.

Another important aspect of our studies is that Rh-CT_{5-HT_{1A}} could functionally and competitively substitute for 5-HT_{1A} signaling responses in hippocampal neurons. Tagging with critical targeting domains to drive differential intracellular localization has, therefore, the potential to induce competitive substitutions of the endogenously expressed proteins. The strategy of targeting domain tagging of exogenous receptors depends on their interaction with chaperone proteins normally binding and trafficking with endogenous receptors. Therefore, exogenously expressed proteins expressed at high enough levels could create an analogous situation to overexpression of the targeting domain alone. This could result in a dominant negative effect by direct competition with endogenous receptors. We reason that this would occur as there are a finite number of trafficking proteins, and

a finite number of positions GPCRs can occupy at a given submembrane locale. Because our goal is to utilize Rh-CT_{5-HT_{1A}} as a functional substitute of 5-HT_{1A}, the pseudo-knockdown of endogenous 5-HT_{1A} signaling would be desirable. For correlative and causal studies linking 5-HT_{1A}-like signaling of Rh-CT_{5-HT_{1A}} to behavior, the compensatory effects from endogenous 5-HT_{1A} signaling would be minimized.

Taken together, our findings suggest that light activation of Rh-CT_{5-HT_{1A}} serves as a suitable proxy for agonist-induced 5-HT_{1A} receptor activation in wild type and 5-HT_{1A} KO animals for understanding the function of 5-HT_{1A} signaling *in*

FIGURE 7. Light activation of Rh-CT_{5-HT_{1A}} functionally rescues 5-HT_{1A} loss-of-function phenotype in cultured hippocampal neurons. *A*, confocal images confirm the lack of 5-HT_{1A} receptors in 5-HT_{1A} KO mice (center-left column). Neurons from wild type (*left column*) and 5-HT_{1A} KO mice (9 DIV) were immunolabeled with anti-5-HT_{1A} (*upper, red*) and anti-MAP-2 (*middle, green*) antibodies. Lower, *left*, overlay shows significant colocalization of 5-HT_{1A} and MAP-2 in wild type neurons (*yellow*). Virally induced 5-HT_{1A}-mCherry and Rh-CT_{5-HT_{1A}} were functionally expressed in the dendrites of cultured hippocampal neurons (9 DIV) of 5-HT_{1A} null mice (*center-right* and *right columns*). Virally transfected KO neurons were stained with anti-dsRed (*upper, red*) and MAP-2 (*middle, green*) antibodies to visualize distribution of mCherry-tagged GPCRs and dendrites, respectively. Exogenously expressed receptors are efficiently expressed and targeted to dendrites. Lower panels, overlay of dsRed and MAP-2 staining reveals a high degree of colocalization of virally transfected 5-HT_{1A}-mCherry and Rh-CT_{5-HT_{1A}} with MAP-2 (*yellow*). *B* and *C*, voltage change induced in cultured hippocampal neurons (10–14 DIV) from wild type mice by baclofen (*B*) and 8OH-DPAT (*C*). *D* and *E*, membrane hyperpolarization is induced in cultured hippocampal neurons (10–14 DIV) from 5-HT_{1A} null mice by baclofen (*D*) but not 8OH-DPAT (*E*). *F* and *G*, agonist (8OH-DPAT) activation of 5-HT_{1A}-mCherry (*F*) and light stimulation of Rh-CT_{5-HT_{1A}} (*G*) expressed in 5-HT_{1A} KO neurons induce hyperpolarization in a similar pattern to the response of wild type neurons to 8OH-DPAT application is shown. *H*, shown is a comparison of the hyperpolarization induced by baclofen, 8OH-DPAT, or light stimulus between KO and wild type neurons in the presence or absence of 5-HT_{1A}-mCherry or Rh-CT_{5-HT_{1A}} (10–14 DIV). *I*, shown is the time course of GPCR (GABA_B, 5-HT_{1A}, 5-HT_{1A}-mCherry, or Rh-CT_{5-HT_{1A}})-induced hyperpolarization and recovery from hyperpolarization after switching off the light or washing out agonist in wild type (WT) and KO mouse neurons (mean \pm S.E.; *, *p* < 0.05, ANOVA).

Chimeric GPCR Controls 5-HT_{1A} Signaling by Light

vitro and *in vivo* preparations. Thus, Rh-CT_{5-HT1A} adds a new engineered GPCR as a tool to control intracellular signaling events.

Acknowledgments—We thank Dr. Lawrence Tecott (University of California, San Francisco) for the 5-HT_{1A} knock-out mice. We also express our gratitude to Dr. Gary Landreth for critically reading the manuscript and providing laboratory space to complete this manuscript.

REFERENCES

1. Stamford, J. A., Davidson, C., McLaughlin, D. P., and Hopwood, S. E. (2000) *Trends Neurosci.* **23**, 459–465
2. Sotelo, C., Cholley, B., El Mestikawy, S., Gozlan, H., and Hamon, M. (1990) *Eur. J. Neurosci.* **2**, 1144–1154
3. Riad, M., Garcia, S., Watkins, K. C., Jodoin, N., Doucet, E., Langlois, X., el Mestikawy, S., Hamon, M., and Descarries, L. (2000) *J. Comp. Neurol.* **417**, 181–194
4. Seletti, B., Benkelfat, C., Blier, P., Annable, L., Gilbert, F., and de Montigny, C. (1995) *Neuropharmacology* **13**, 93–104
5. Leone, M., Attanasio, A., Croci, D., Ferraris, A., D'Amico, D., Grazzi, L., Nespolo, A., and Buscone, G. (1998) *Neuroreport* **9**, 2605–2608
6. Raymond, J. R., Mukhin, Y. V., Gelasco, A., Turner, J., Collinsworth, G., Gettys, T. W., Grewal, J. S., and Garnovskaya, M. N. (2001) *Pharmacol. Ther.* **92**, 179–212
7. Lanfumey, L., and Hamon, M. (2004) *Curr. Drug Targets CNS Neurol. Disord.* **3**, 1–10
8. Herlitze, S., and Landmesser, L. T. (2007) *Curr. Opin. Neurobiol.* **17**, 87–94
9. Li, X., Gutierrez, D. V., Hanson, M. G., Han, J., Mark, M. D., Chiel, H., Hegemann, P., Landmesser, L. T., and Herlitze, S. (2005) *Proc. Natl. Acad. Sci. U.S.A.* **102**, 17816–17821
10. Wittemann, S., Mark, M. D., Rettig, J., and Herlitze, S. (2000) *J. Biol. Chem.* **275**, 37807–37814
11. Bekkers, J. M., and Stevens, C. F. (1991) *Proc. Natl. Acad. Sci. U.S.A.* **88**, 7834–7838
12. Xie, M., Li, X., Han, J., Vogt, D. L., Wittemann, S., Mark, M. D., and Herlitze, S. (2007) *J. Cell Biol.* **178**, 489–502
13. Heisler, L. K., Chu, H. M., Brennan, T. J., Danao, J. A., Bajwa, P., Parsons, L. H., and Tecott, L. H. (1998) *Proc. Natl. Acad. Sci. U.S.A.* **95**, 15049–15054
14. Parsons, L. H., Kerr, T. M., and Tecott, L. H. (2001) *J. Neurochem.* **77**, 607–617
15. Scott-McKean, J. J., Wenger, G. R., Tecott, L. H., and Costa, A. C. (2008) *Open Neuropsychopharmacol. J.* **1**, 24–32
16. Lerch-Haner, J. K., Frierson, D., Crawford, L. K., Beck, S. G., and Deneris, E. S. (2008) *Nat. Neurosci.* **11**, 1001–1003
17. Li, X., Hümmer, A., Han, J., Xie, M., Melnik-Martinez, K., Moreno, R. L., Buck, M., Mark, M. D., and Herlitze, S. (2005) *J. Biol. Chem.* **280**, 23945–23959
18. Hamill, O. P., Marty, A., Neher, E., Sakmann, B., and Sigworth, F. J. (1981) *Pflügers Arch.* **391**, 85–100
19. Carrel, D., Masson, J., Al Awabdh, S., Capra, C. B., Lenkei, Z., Hamon, M., Emerit, M. B., and Darmon, M. (2008) *J. Neurosci.* **28**, 8063–8073
20. Moritz, O. L., Tam, B. M., Papermaster, D. S., and Nakayama, T. (2001) *J. Biol. Chem.* **276**, 28242–28251
21. Jin, S., McKee, T. D., and Oprian, D. D. (2003) *FEBS Lett.* **542**, 142–146
22. Perkins, B. D., Fadol, J. M., and Dowling, J. E. (2004) *Methods Cell Biol.* **76**, 315–331
23. Melia, T. J., Jr., Cowan, C. W., Angleson, J. K., and Wensel, T. G. (1997) *Biophys. J.* **73**, 3182–3191
24. Shaner, N. C., Campbell, R. E., Steinbach, P. A., Giepmans, B. N., Palmer, A. E., and Tsien, R. Y. (2004) *Nat. Biotechnol.* **22**, 1567–1572
25. Lamb, T. D., and Pugh, E. N., Jr. (2004) *Prog. Retin Eye Res.* **23**, 307–380
26. Brueggemann, L. I., and Sullivan, J. M. (2002) *J. Gen. Physiol.* **119**, 593–612
27. Cornwall, M. C., and Fain, G. L. (1994) *J. Physiol.* **480**, 261–279
28. Fain, G. L., Matthews, H. R., and Cornwall, M. C. (1996) *Trends Neurosci.* **19**, 502–507
29. Cornwall, M. C., Matthews, H. R., Crouch, R. K., and Fain, G. L. (1995) *J. Gen. Physiol.* **106**, 543–557
30. Kim, J. M., Hwa, J., Garriga, P., Reeves, P. J., RajBhandary, U. L., and Khorana, H. G. (2005) *Biochemistry* **44**, 2284–2292
31. Airan, R. D., Thompson, K. R., Fenno, L. E., Bernstein, H., and Deisseroth, K. (2009) *Nature* **458**, 1025–1029
32. Kia, H. K., Miquel, M. C., Brisorgueil, M. J., Daval, G., Riad, M., El Mestikawy, S., Hamon, M., and Vergé, D. (1996) *J. Comp. Neurol.* **365**, 289–305
33. Kim, J., Dittgen, T., Nimmerjahn, A., Waters, J., Pawlak, V., Helmchen, F., Schlesinger, S., Seeburg, P. H., and Osten, P. (2004) *J. Neurosci. Methods* **133**, 81–90
34. Mark, M. D., and Herlitze, S. (2000) *Eur. J. Biochem.* **267**, 5830–5836
35. Li, Z., Zhuang, J., and Corson, D. W. (1999) *Photochem. Photobiol.* **69**, 500–504
36. Coward, P., Wada, H. G., Falk, M. S., Chan, S. D., Meng, F., Akil, H., and Conklin, B. R. (1998) *Proc. Natl. Acad. Sci. U.S.A.* **95**, 352–357
37. Armbuster, B. N., Li, X., Pausch, M. H., Herlitze, S., and Roth, B. L. (2007) *Proc. Natl. Acad. Sci. U.S.A.* **104**, 5163–5168
38. Pei, Y., Rogan, S. C., Yan, F., and Roth, B. L. (2008) *Physiology* **23**, 313–321
39. Zemelman, B. V., Lee, G. A., Ng, M., and Miesenbock, G. (2002) *Neuron* **33**, 15–22